LF Groundwave Propagation Modeling Over Irregular Terrain by the Hybrid Two-Way Parabolic Equation Method

Dan-Dan Wang, Xiao-Li Xi, *Member, IEEE*, Yu-Rong Pu, Jin-Sheng Zhang, and Li-Li Zhou

***Abstract*— The traditional two-way (2W) parabolic equation (PE) (2W-PE) method has been applied for modeling groundwave propagation over irregular terrain. However, based on a staircase terrain model (STM), the method is not sufficient in sloping facets modeling. Although more accurate one-way PE method based on conformal mapping model (CMM) is available, it handles only forward-propagating waves and neglects the backward-propagating waves, which become significant especially for steep terrain. In this paper, a hybrid 2W-PE method is presented to model the low-frequency (LF) groundwave propagation over irregular terrain. The method combines the STM and CMM to improve the prediction accuracy of both forward and backward propagations. The numerical results are compared with those of the conventional 2W-PE and finite-difference time-domain (FDTD) methods. While calibrated against the FDTD method, the proposed hybrid 2W-PE method has higher accuracy than the traditional 2W-PE method at the same computational cost.**

***Index Terms*— Conformal mapping model (CMM), irregular terrain, low-frequency (LF) groundwave propagation, staircase terrain model (STM), two-way parabolic equation (2W-PE) method.**

I. Introduction

LOW-FREQUENCY (LF) radio waves have long been used for ground-based positioning, navigation, and timing (PNT) in many countries. In use on the ground, disturbances resulted from topographic irregularities and changes in conductivity cause significant errors [1]. Over the years, three approaches for predicting the terrain effects on the amplitude and phase of the LF groundwave have evolved: i.e., the finite-difference time-domain (FDTD) [2]–[5], integral equation (IE) [6], [7], and parabolic equation (PE) [8]–[12] methods. The FDTD method provides an accurate full-wave solution for irregular propagation paths, but it suffers from huge computational expenses for large-scale problems. The IE and PE methods belong to the efficient one-way propagation model, which, by nature, handles only forward-propagating waves and, hence, omits the backward-propagating waves. This may cause errors, especially in the case when strong backward-propagating waves occur during propagation over irregular terrain. Hence, there is a need for a two-way (2W) propagation model that considers both forward- and backward-propagating waves for large-scale scattering problems.

The 2W PE (2W-PE) method was first proposed by Collins and Evans [13] for acoustic backscattering problems. Later on, much of pioneer works have been done to extend the 2W-PE method in the areas including acoustic backscattering problems [14], [15] and multiple knife-edges' scattering problems [16], [17]. Recently, a 2W split-step (SS) PE (2W-SSPE) method has been proposed for modeling multipath reflection effects over a staircase-approximated terrain in troposphere [18] and then tested and calibrated against analytical solutions and other numerical methods [19]–[21]. In [22] and [23], a 2W finite-element (FEM) PE (2W-FEMPE) method was developed for groundwave propagation modeling in the UHF band. The main advantage of the 2W-FEMPE method over the 2W-SSPE method is the easiness in handling arbitrary boundary conditions (BCs). However, the 2W-SSPE method has been used in most long-range propagation problems due to its efficiency and robustness. In [24], the SS algorithm-based 2W-PE method was applied for the calculation of propagation loss in urban environments. Most recently, Ahdab and Akleman [25] proposed a 3-D 2W-PE method for radio wave propagation analysis [25], but the method is only applicable to perfectly electrical conducting surfaces.

The existing 2W-PE methods are based on the staircase terrain model (STM) with limitations for hills or valleys since the BCs on sloping facets are approximated. On the other hand, the conformal mapping model (CMM)-based PE method is more accurate for modeling sloping facets, but it cannot capture the backward-propagating waves from obstacles.

Manuscript received May 11, 2018; revised April 22, 2019; accepted June 9, 2019. Date of publication July 2, 2019; date of current version October 4, 2019. This work was supported in part by the National Natural Science Foundation of China under Grant 61771389, in part by the Preresearch Foundation of Weapons Equipment of China under Grant 61405180202, in part by the Shaanxi Key Laboratory of Complex System Control and Intelligent Information Processing of Xi'an University of Technology under Grant 2017CP08, and in part by the Doctoral Innovation Fund of the Xi'an University of Technology under Grant 310-252071710. *(Corresponding author: Xiao-Li Xi.)*

D.-D. Wang, X.-L. Xi, and Y.-R. Pu are with the Faculty of Automation and Information Engineering, Xi'an University of Technology, Xi'an 710048, China (e-mail: xixiaoli@xaut.edu.cn).

J.-S. Zhang is with the Faculty of Automation and Information Engineering, Xi'an University of Technology, Xi'an 710048, China, and also with the Xi'an High-Tech Institute, Xi'an 710025, China.

L.-L. Zhou is with the Shaanxi Key Laboratory of Complex System Control and Intelligent Information Processing, Xi'an University of Technology, Xi'an 710048, China, and also with the College of Electrical and Information Engineering, Shaanxi University of Science and Technology, Xi'an 710021, China.

Color versions of one or more of the figures in this article are available online at http://ieeexplore.ieee.org.

Digital Object Identifier 10.1109/TAP.2019.2925155

In this paper, we present a hybrid 2W-PE method for the modeling of LF groundwave propagation in the presence of irregular terrain, which combines the STM and CMM to improve the accuracy of both forward and backward propagation predictions. The initial reflected field by the obstacles is first calculated using the STM and then applied to the forward–backward CMM procedure to propagate the field on the sloping facets properly. The use of the SS Fourier algorithm in the implementation of the hybrid method ensures an efficient calculation. The accuracy and efficiency of the hybrid 2W-PE method are demonstrated by representative numerical examples. For the sake of completeness, both the amplitude and phase results of LF groundwave are considered.

II. Traditional 2W-PE Model

A. 2W-PE Formulation

Derivations of the forward and backward PEs from the Helmholtz equation have been previously published in [8] and [18] and will not be repeated here. Under $e^{-i\omega t}$ time dependence, assuming the field components being independent of azimuth (φ), the forward and backward PEs are given by [8]

$$\frac{\partial u_f(\rho,z)}{\partial \rho} = \frac{ik_0}{2}\left[\frac{1}{k_0^2}\frac{\partial^2}{\partial z^2} + (n^2-1)\right] u_f(\rho,z) \quad (1)$$

$$\frac{\partial u_b(\rho,z)}{\partial \rho} = -\frac{ik_0}{2}\left[\frac{1}{k_0^2}\frac{\partial^2}{\partial z^2} + (n^2-1)\right] u_b(\rho,z) \quad (2)$$

where ρ and z are the cylindrical coordinates corresponding to the range and height, respectively, k_0 is the wave number in free space, n is the refractive index, and u_f and u_b denote the forward and backward auxiliary fields, respectively. The relation between the auxiliary fields and the field components can be expressed as follows:

$$u_f(\rho,z) = \sqrt{k_0\rho}\, e^{-ik_0\rho}\Phi_f(\rho,z) \quad (3)$$

$$u_b(\rho,z) = \sqrt{k_0\rho}\, e^{ik_0\rho}\Phi_b(\rho,z) \quad (4)$$

where Φ_f and Φ_b represent the forward and backward fields (magnetic (electric) field for vertical (horizontal) polarization), respectively.

The numerical solutions of both forward and backward PEs can be obtained by the efficient SS Fourier algorithm proposed in [9]

$$u_f(\rho+\Delta\rho,z) = e^{\frac{ik_0(n^2-1)\Delta\rho}{2}}\Im^{-1}\left\{e^{\frac{-ip^2\Delta\rho}{2k_0}}\Im\{u_f(\rho,z)\}\right\} \quad (5)$$

$$u_b(\rho-\Delta\rho,z) = e^{\frac{ik_0(n^2-1)\Delta\rho}{2}}\Im^{-1}\left\{e^{\frac{-ip^2\Delta\rho}{2k_0}}\Im\{u_b(\rho,z)\}\right\} \quad (6)$$

where $\Im$ and $\Im^{-1}$ denote the discrete mixed Fourier transform (DMFT) [9] pair, and the transform variable p is defined by $k_0\sin\theta$, where θ is the propagation angle and $\Delta\rho$ is the range step. The basic idea of the DMFT is to match the PE algorithm to the impedance BC [8], [9]. It is seen from (5) and (6) that u_f and u_b can be calculated through the same marching procedure.

B. Initial Field

The 2W-PE method represents an initial-value problem. The initial forward field is solved by the flat-earth formula (FEF) [12], [26]. The FEF provides the analytical solution for the calculation of the electromagnetic field of a vertical electric dipole with the electric moment Idl at the height d over the earth. For brevity, only the magnetic field in the air is listed here [26]

$$H_\varphi = -\frac{Idl}{2\pi}\left[\frac{e^{ik_0r_1}}{2}\left(\frac{\rho}{r_1}\right)\left(\frac{ik_0}{r_1}-\frac{1}{r_1^2}\right)+\frac{e^{ik_0r_2}}{2}\left(\frac{\rho}{r_2}\right)\times\left(\frac{ik_0}{r_2}-\frac{1}{r_2^2}\right)-e^{ik_0r_2}\frac{k_0^3}{k_1}\left(\frac{\pi}{k_0r_2}\right)^{1/2}e^{-iP}F(P)\right] \quad (7)$$

where

$$F(P) = \int_P^\infty \frac{e^{it}}{\sqrt{2\pi t}}dt \quad (8)$$

$$r_1 = [\rho^2+(z-d)^2]^{1/2};\quad r_2 = [\rho^2+(z+d)^2]^{1/2} \quad (9)$$

$$P = \frac{k_0^3r_2}{2k_1^2}\left(\frac{k_0r_2+k_1(z+d)}{k_0\rho}\right)^2 \quad (10)$$

and k_1 is the wave number of the earth. We always have $|k_1|^2 >> k_0^2$. Then, the initial forward field Φ_f at $\rho=\rho_0$ can be calculated using (7).

Suppose that the initial forward field is marched out in the forward direction until reaching a vertical terrain facet located at $\rho=\rho_e$. The partially reflected forward field by the vertical terrain facet generates the initial backward field, which can be calculated by imposing the BC on the facet

$$u_b(\rho_e,z) = \begin{cases} 0, & z > T(\rho_e) \\ Ru_f(\rho_e,z)e^{i2k_0\rho_e}, & T(\rho_e-\Delta\rho) < z < T(\rho_e) \end{cases} \quad (11)$$

where $T(\rho)$ is the terrain height and R is the reflection coefficient on the terrain facet.

C. Implementation of the 2W-PE Algorithm

The implementation of the traditional 2W-PE algorithm will be briefly described here, but the reader is referred to [18] and [21] for a more detailed illustration of the algorithm. The main idea of the algorithm is as follows [18]–[21]: when the propagating field hits an uphill obstacle, the vertical field is split into forward and backward components by imposing appropriate BCs. On the vertical terrain facet, the forward component is simply eliminated; the backward field is initiated from the forward field and then propagated reversely. After passing the obstacle, the downhill fields propagate in the usual manner. Multiple reflections are treated iteratively in the same way. This method is accurate if the terrain has a staircasing shape [8], which is rarely the case. For sloping terrains such as hills or valleys, errors occur due to the staircase approximation of the facets [21].

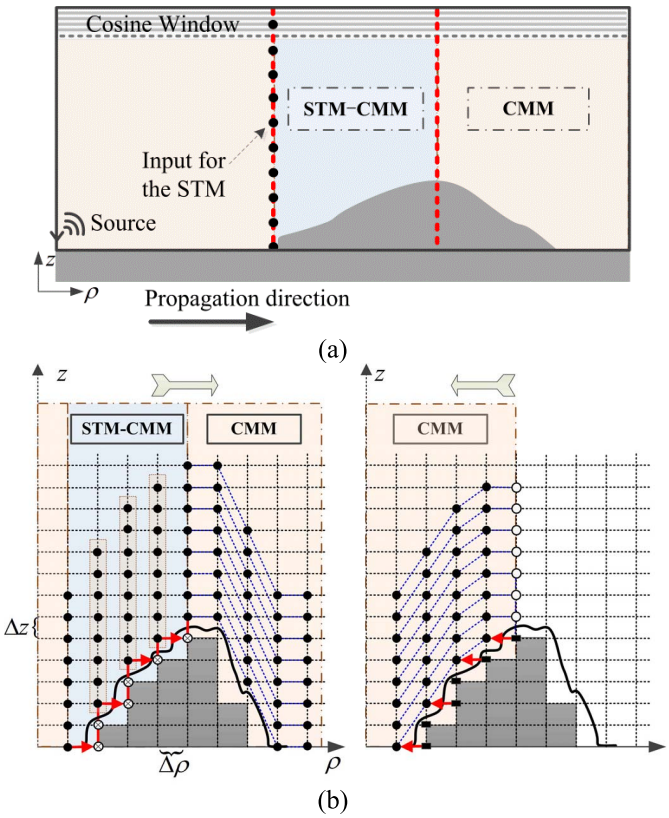

Fig. 1. Sketch of the hybrid 2W-PE model. (a) Simulation model. (b) Forward-propagating waves (left) and backward-propagating waves (right). (● denotes nonzero fields, ⊗ represents the field truncated according to the vertical terrain facet, ○ represents the zero fields to remain the DMFT grid, and ■ denotes the initial backward field generated from terrain reflections.)

III. Hybrid 2W-PE Model

A. Scenario of the Hybrid 2W-PE Model

Fig. 1 shows the sketch of the proposed hybrid 2W-PE method for irregular terrain modeling based on a combination of STM and CMM. The simulation space is divided into two regions: a combined STM–CMM region (uphill) and a pure CMM (downhill/flat) region. In the combined region, two sets of field representations based on STM and CMM coexist, the STM is employed to solve the reflected initial field at the vertical terrain facets in the usual manner, while the CMM is used to properly march out and back the field on the sloping facets. In addition, the field at the boundary of the pure CMM region serves as the input for the STM of the combined region. The initial reflected field is first solved by the STM, then coupled into the CMM. Following this approach, higher accuracy is obtained both before and after the obstacles.

The hybrid algorithm can also be extended for the estimation of the multiple reflections following the procedure described in [18]–[22]. Each time when the wave strikes at a vertical terrain facet, it is split into a forward and a backward component. The total field Φ at each range step is achieved by the superposition of the forward and backward fields. Note that the wave in the region between the obstacles bounces recursively from each other. The iteratively marching algorithm is repeated until a certain threshold criterion is achieved (i.e., $\|\Phi^n - \Phi^{n-1}\|/\|\Phi^{n-1}\| < \varepsilon$, where $\|\cdot\|$ denotes the Euclidian norm, Φ^n and Φ^{n-1} are the total fields at the n^{th} and $(n-1)^{\text{th}}$ steps, respectively, and ε is the threshold).

B. 2W-PE Formulation Based on CMM

Using the terrain flattening transformation [10], we define the new range and height variables by

$$\begin{cases} \chi = \rho \\ \zeta = z - T(\rho). \end{cases} \tag{12}$$

The forward and backward auxiliary fields u_f and u_b, respectively, are transformed into the shifted coordinate system as

$$u_f(\rho, z) = \Psi_f(\chi, \zeta) e^{i\vartheta_f(\chi,\zeta)} \tag{13}$$

$$u_b(\rho, z) = \Psi_b(\chi, \zeta) e^{i\vartheta_b(\chi,\zeta)} \tag{14}$$

where $\vartheta_f(\chi, \zeta)$ and $\vartheta_b(\chi, \zeta)$ are yet to be determined. Substituting (13) into (1), and (14) into (2), we have

$$\frac{\partial \Psi_f(\chi,\zeta)}{\partial \chi} = \frac{ik_0}{2}\left[\frac{1}{k_0^2}\frac{\partial^2}{\partial \zeta^2} + (m^2 - 1)\right]\Psi_f(\chi,\zeta) \tag{15}$$

$$\frac{\partial \Psi_b(\chi,\zeta)}{\partial \chi} = -\frac{ik_0}{2}\left[\frac{1}{k_0^2}\frac{\partial^2}{\partial \zeta^2} + (m^2 - 1)\right]\Psi_b(\chi,\zeta) \tag{16}$$

where $m^2 = n^2(\chi, \zeta + T(\chi)) - 2\zeta T''(\chi)$, $T''(\chi)$ represents the second derivative with respect to χ. In the limit $T''(\chi) = 0$ (flat surface), (15) and (16) reduced to the forward and backward PEs in (1) and (2). $\vartheta_f(\chi, \zeta)$ and $\vartheta_b(\chi, \zeta)$ are derived as

$$\vartheta_f(\chi,\zeta) = k_0\zeta T'(\chi) + \frac{k_0}{2}\int_0^{\chi} [T'(s)]^2 ds \tag{17}$$

$$\vartheta_b(\chi,\zeta) = -\vartheta_f(\chi,\zeta). \tag{18}$$

In the shifted coordinate system, following the SS Fourier algorithm in [9] and [10], we have:

$$\Psi_f(\chi + \Delta\chi, \zeta) = e^{\frac{ik_0(m^2-1)\Delta\chi}{2}} \Im^{-1}\left\{e^{\frac{-ip^2\Delta\chi}{2k_0}} \Im\{\Psi_f(\chi,\zeta)\}\right\} \tag{19}$$

$$\Psi_b(\chi - \Delta\chi, \zeta) = e^{\frac{ik_0(m^2-1)\Delta\chi}{2}} \Im^{-1}\left\{e^{\frac{-ip^2\Delta\chi}{2k_0}} \Im\{\Psi_b(\chi,\zeta)\}\right\}. \tag{20}$$

Similarly, it is observed from (19) and (20) that Ψ_f and Ψ_b can be calculated by iteration processes once the initial forward and backward fields are determined. Transforming Ψ_f and Ψ_b back to the (ρ, z) coordinate system, the forward and backward fields are calculated using (3) and (4).

IV. Numerical Results

In this section, we present two representative numerical examples to demonstrate the accuracy and efficiency of the hybrid 2W-PE method with the narrow-angle version. For each example, a 100 kHz vertical electric dipole is placed at the coordinate origin with a radiation power of 1 kW. The electric parameters of the ground are taken as $\varepsilon_r = 13$ and $\sigma = 3 \times 10^{-3}$ S/m [3]. The height function of a Gaussian-shaped mountain is given by

$$T(\rho) = H \exp\{-9[(\rho - \rho_c)/l]^2\} \tag{21}$$

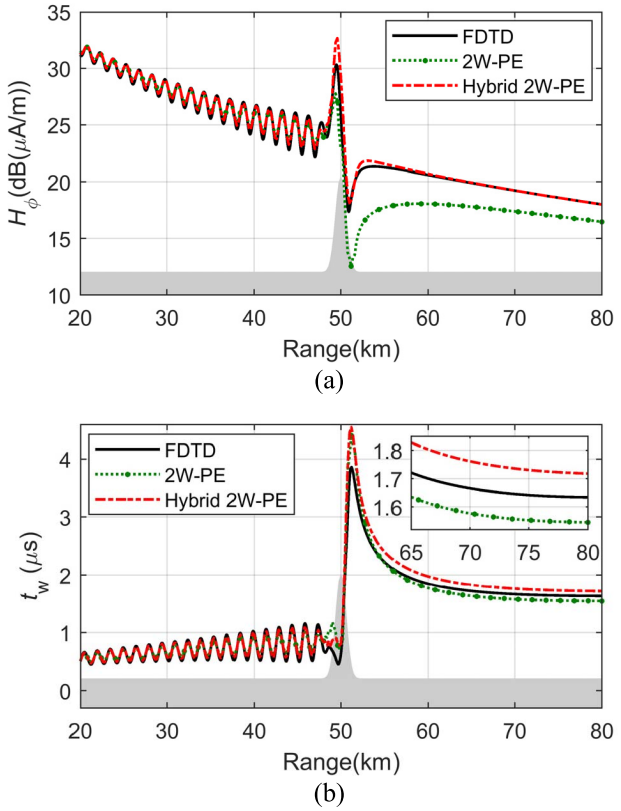

Fig. 2. Comparison of the (a) magnetic field strength and (b) secondary time delay of the hybrid 2W-PE algorithm with those of STM-based 2W-PE and FDTD methods over a steep mountain path on the ground.

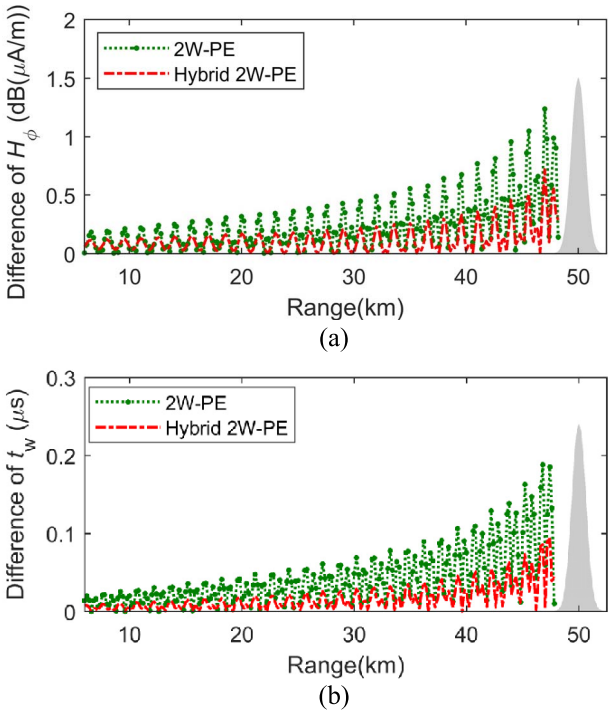

Fig. 3. Differences in the (a) magnetic field strength and (b) secondary time delay computed by the STM-based 2W-PE and hybrid 2W-PE methods calibrated against the FDTD method in the front of the mountain.

where H is the mountain height, ρ_c is the distance from the transmitter to the center of the mountain, and l is the parameter controlling the real mountain width L and $L \approx 1.25l$ [4], [5]. As no exact analytical solution is available for such an irregular terrain, the numerical FDTD method with fine mesh can be taken as a reference solution. The gird sizes for the FDTD method are defined as $\Delta\rho = \Delta z = 10$ m. Its time step Δt is 16.667 ns according to the Courant stability limit. For the PE methods, the range and height increments are $\Delta\rho = 200$ m and $\Delta z = 50$ m, respectively.

In LF groundwave applications, two key parameters are of interests: the field strength Φ and the secondary time delay t_w [3]–[6]. We evaluate both for all methods considered herein, and their definitions are repeated below.

The field strength for a vertical dipole regarding the radiated power P_t is expressed as [6]

$$\Phi(\text{dB}) = \Phi \times \frac{1}{k_0}\sqrt{\frac{P_t}{40}} \tag{22}$$

for both the time-domain and frequency-domain methods, where Φ on the right side of (22) represents the steady-state field component.

The secondary time delay for a time-domain method is given by [3]

$$t_w = t_0 - \frac{\rho}{c} \tag{23}$$

where t_0 is the arrival time of the signal, and ρ/c represents the time delay in free-space. The secondary time delay indicates the excess time delay over free-space. For a frequency-domain method, the secondary time delay is calculated through the phase of groundwave attenuation factor [6]. The attenuation factor W is defined by

$$W = \Phi/\Phi_0 \tag{24}$$

where Φ represents the field strength in the presence of actual path and Φ_0 represents the free space field strength. The phase of W is directly related to the secondary time delay [6]

$$t_w = \arg W/\omega \tag{25}$$

where ω is the angular frequency of the source in rad/s.

The first example involves wave propagation over a steep mountain to illustrate the accuracy of the hybrid 2W-PE method. Here, a 100 km-long propagation path is used, with a 3.125 km-long, 1.5 km-high Gaussian-shaped mountain centered at a distance of 50 km from the transmitter. Fig. 2 compares the magnetic field strength H_φ and the secondary time delay t_w results with those of the traditional 2W-PE and the FDTD methods on the ground. As shown in Fig. 2, using the 2W-PE algorithms, strong interferences of the forward and backward waves in both the amplitude and phase are captured. Also, the interferences decrease with increasing distance to the mountain. We take a closer look at the accuracies of the two 2W-PE methods. For better visualization, we plot the differences, between each PE and FDTD, of H_φ and t_w in Fig. 3. The difference is defined by $|\phi - \phi_{\text{fdtd}}|$, where ϕ represents the numerical results calculated by the PE methods, and ϕ_{fdtd} is the reference solution using FDTD. It is noted that the hybrid 2W-PE method gives higher amplitude and phase accuracy than the traditional 2W-PE method before the

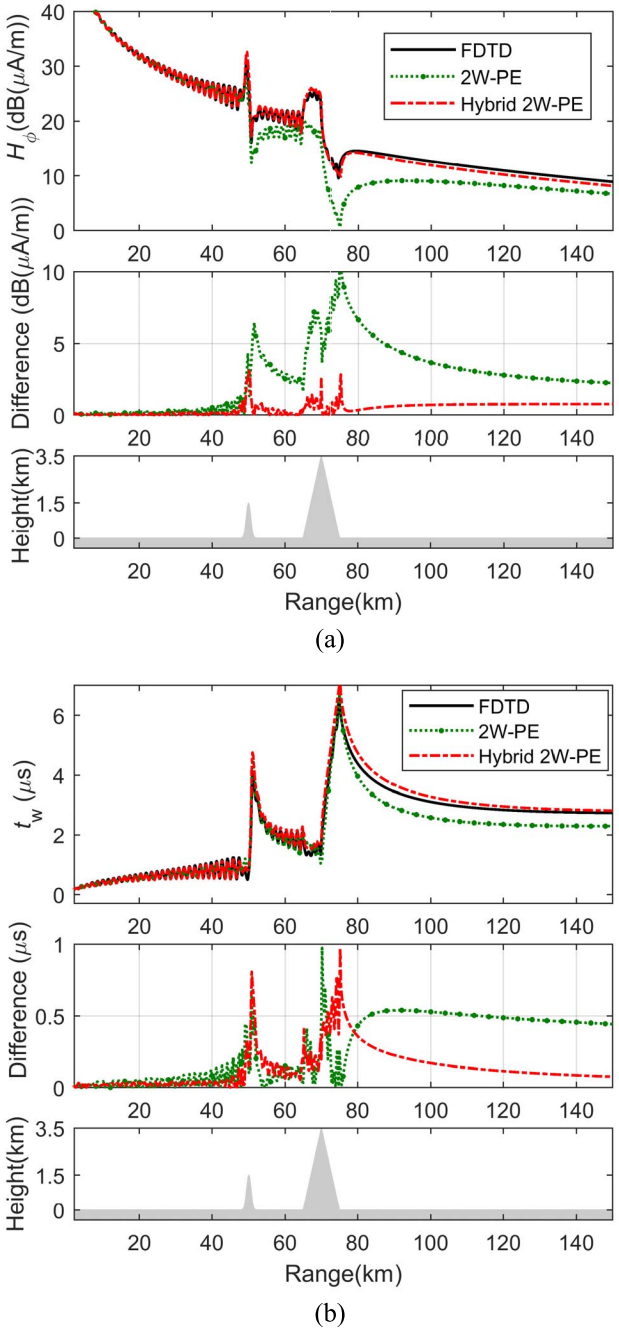

Fig. 4. Comparison of the (a) magnetic field strength and (b) secondary time delay as a function of range over a two-mountain path on the ground.

mountain region. After the mountain region, the amplitude results of the hybrid 2W-PE and the FDTD methods are very close but differ from the traditional 2W-PE method due to the staircase approximation. The phase errors of the two 2W-PE methods are on the same level referring to the FDTD result.

In the second example, we further test a 150 km-long propagation path with two separate mountains to show the efficiency of the hybrid algorithm. The first mountain has a Gaussian shape, located 50 km away from the transmitter, with a width of 3.125 km and a height of 1.5 km. The second triangle-shaped mountain with a width of 10 km and a height of 3.5 km is 20 km away from the first mountain.

TABLE I

COMPUTATIONAL COST COMPARISON OF THE FDTD, 2W-PE, AND HYBRID 2W-PE METHODS

Method	Time(s)	Memory(MB)
FDTD-CUDA	2280.000	658.00
2W-PE	66.441	34.93
Hybrid 2W-PE	73.925	38.57

The threshold ε is 0.025 [21]. Fig. 4 shows the comparison of the hybrid 2W-PE, the traditional 2W-PE, and the FDTD results on the ground. It is seen that the hybrid 2W-PE method significantly improves the accuracy of the traditional 2W-PE method, especially in the amplitude.

In this paper, the FDTD program is parallelly implemented on the graphics processing unit (GPU) (Nvidia GeForce GTX960) with 1024 cores. Specifically for the second example, the FDTD domain has $15\,300 \times 1000$ cells, $35\,000$ time steps. The 2W-PE domain is defined by 751×2048 cells. Table I lists the computational time and memory comparison of the three methods. As shown here, the two 2W-PE methods have the same level of computational cost. Note that the FDTD method is taken as a reference solution for the accuracy investigation of the PE methods. The single-frequency nature of the problem we study here does not demonstrate the advantages of the FDTD as a time-domain method.

V. CONCLUSION

In this paper, a hybrid 2W-PE method has been presented to predict LF groundwave propagation in the presence of irregular terrain. Tests and comparisons were done systematically against the conventional 2W-PE method. The FDTD results were taken as references for calibration purpose. The numerical results showed that the hybrid algorithm achieves higher accuracy than the traditional one with little extra computational cost.

Furthermore, note that the hybrid 2W-PE method has an intrinsic limitation associated with its narrow-angle version. Usually, this limitation does not prevent the method to give accurate results for most of the long-range groundwave propagation problems. Future research concerning multiple reflections and diffractions at large propagation angles because of steep terrain necessitates an extension of the presented method to a wide-angle version. Nevertheless, we found that none of the existing CMM-based PEs have a wide-angle capability. Particularly, the performance of the narrow-angle CMM-based PE method is almost not affected by the terrain slope, whereas for its wide-angle version, the wide-angle capability deteriorates dramatically as the terrain slope increases. Detailed analysis of the narrow-angle and wide-angle CMM-based PE methods, however, is beyond the scope of this paper and will be presented in future publications.

REFERENCES

[1] J. M. Ross and J. E. Kirch, "A few observations of the perturbations in the phase of the low-frequency ground wave," *J. Res. Nat. Bureau Standards. Sect. D, Radio Propag.*, vol. 65D, no. 4, pp. 393–396, Mar. 1961.

[2] A. Taflove, *Computational Electrodynamics: The Finite-Difference Time-Domain Method*. Boston, MA, USA: Artech House, 1995.

[3] X. Xi, L. Zhou, J. Zhang, J. Liu, and L. Wang, "Combined IE-FDTD algorithm for long-range loran-C ground-wave propagation," *IEEE Trans. Antennas Propag.*, vol. 60, no. 8, pp. 3802–3808, Aug. 2012.
[4] L. Zhou, X. Xi, J. Zhang, and Y. Pu, "A new method for loran-C ASF calculation over irregular terrain," *IEEE Trans. Aerosp. Electron. Syst.*, vol. 49, no. 3, pp. 1738–1744, Jul. 2013.
[5] L. Zhou, X. Xi, J. Liu, and N. Yu, "LF ground-wave propagation over irregular terrain," *IEEE Trans. Antennas Propag.*, vol. 59, no. 4, pp. 1254–1260, Apr. 2011.
[6] T. S. M. Maclean and Z. Wu, *Radiowave Propagation over Ground*. London, U.K.: Chapman & Hall, 1993.
[7] H. Gesny and O. Ravard, "Propagation over irregular terrain in the VHF band: A review of integral equation models," in *Proc. IEE Nat. Conf. Antennas Propag.*, Mar./Apr. 1999, pp. 61–64.
[8] M. Levy, *Parabolic Equation Methods for Electromagnetic Wave Propagation*. London, U.K.: The Institution of Electrical Engineers, 2000.
[9] D. Dockery and J. R. Kuttler, "An improved impedance-boundary algorithm for Fourier split-step solutions of the parabolic wave equation," *IEEE Trans. Antennas Propag.*, vol. 44, no. 12, pp. 1592–1599, Dec. 1996.
[10] A. E. Barrios, "A terrain parabolic equation model for propagation in the troposphere," *IEEE Trans. Antennas Propag.*, vol. 42, no. 1, pp. 90–98, Jan. 1994.
[11] G. Apaydin and L. Sevgi, "Numerical investigations of and path loss predictions for surface wave propagation over sea paths including hilly island transitions," *IEEE Trans. Antennas Propag.*, vol. 58, no. 4, pp. 1302–1314, Apr. 2010.
[12] D.-D. Wang, X.-L. Xi, Y.-R. Pu, J.-F. Liu, and L.-L. Zhou, "Parabolic equation method for Loran-C ASF prediction over irregular terrain," *IEEE Antennas Wireless Propag. Lett.*, vol. 15, pp. 734–737, 2016.
[13] M. D. Collins and R. B. Evans, "A two-way parabolic equation for acoustic backscattering in the ocean," *J. Acoust. Soc. Amer.*, vol. 91, no. 3, pp. 1357–1368, 1992.
[14] M. D. Collins, "A two-way parabolic equation for elastic media," *J. Acoust. Soc. Amer.*, vol. 93, no. 4, pp. 1815–1825, 1993.
[15] J. F. Lingevitch, M. D. Collins, M. J. Mills, and R. B. Evans, "A two-way parabolic equation that accounts for multiple scattering," *J. Acoust. Soc. Amer.*, vol. 112, no. 2, pp. 476–480, 2002.
[16] M. J. Mills, M. D. Collins, and J. F. Lingevitch, "Two-way parabolic equation techniques for diffraction and scattering problems," *Wave Motion*, vol. 31, no. 2, pp. 173–180, 2000.
[17] H. Oraizi and S. Hosseinzadeh, "Radio-wave-propagation modeling in the presence of multiple knife edges by the bidirectional parabolic-equation method," *IEEE Trans. Veh. Technol.*, vol. 56, no. 3, pp. 1033–1040, May 2007.
[18] O. Ozgun, "Recursive two-way parabolic equation approach for modeling terrain effects in tropospheric propagation," *IEEE Trans. Antennas Propag.*, vol. 57, no. 9, pp. 2706–2714, Sep. 2009.
[19] O. Ozgun, G. Apaydin, M. Kuzuoglu, and L. Sevgi, "Two-way Fourier split step algorithm over variable terrain with narrow and wide angle propagators," in *Proc. IEEE Antennas Propag. Soc. Int. Symp.*, Toronto, ON, Canada, Jul. 2010, pp. 1–4.
[20] O. Ozgun, M. Kuzuoglu, G. Apaydin, and L. Sevgi, "Two-way split-step parabolic equation algorithm for tropospheric propagation: Tests and comparisons," in *Proc. 10th Medit. Microw. Symp.*, Aug. 2010, pp. 14–17.
[21] O. Ozgun, G. Apaydin, M. Kuzuoglu, and L. Sevgi, "PETOOL: MATLAB-based one-way and two-way split-step parabolic equation tool for radiowave propagation over variable terrain," *Comput. Phys. Commun.*, vol. 182, no. 12, pp. 2638–2654, Dec. 2011. [Online]. Available: http://cpc.cs.qub.ac.uk/summaries/AEJS_v1_0.html
[22] G. Apaydin, O. Ozgun, M. Kuzuoglu, and L. Sevgi, "A novel two-way finite-element parabolic equation groundwave propagation tool: Tests with canonical structures and calibration," *IEEE Trans. Geosci. Remote Sens.*, vol. 49, no. 8, pp. 2887–2899, Aug. 2011.
[23] G. Apaydin, O. Ozgun, M. Kuzuoglu, and L. Sevgi, "Two-way split-step Fourier and finite element based parabolic equation propagation tools: Comparisons and calibration," in *Proc. IEEE Antennas Propag. Soc. Int. Symp.*, Toronto, ON, Canada, Jul. 2010, pp. 1–4.
[24] K. Wang and Y. Long, "Propagation modeling over irregular terrain by the improved two-way parabolic equation method," *IEEE Trans. Antennas Propag.*, vol. 60, no. 9, pp. 4467–4471, Sep. 2012.
[25] Z. El Ahdab and F. Akleman, "Radiowave propagation analysis with a bidirectional 3-D vector parabolic equation method," *IEEE Trans. Antennas Propag.*, vol. 65, no. 4, pp. 1958–1966, Apr. 2017.
[26] R. W. P. King and S. S. Sandler, "The electromagnetic field of a vertical electric dipole over the Earth or sea," *IEEE Trans. Antennas Propag.*, vol. 42, no. 3, pp. 382–389, Mar. 1994.

Dan-Dan Wang received the B.S. and M.S. degrees in electronic engineering from the Xi'an University of Technology, Xi'an, China, in 2013 and 2016, respectively, where she is currently pursuing the Ph.D. degree in electronic engineering.

Her current research interests include wave propagation and numerical calculation of electromagnetic fields.

Xiao-Li Xi (M'10) received the B.S. degree in applied physics from the University of Defense Technology, Changsha, China, in 1990, the M.S. degree in biomedical engineering from Fourth Military Medical University, Xi'an, China, in 1998, and the Ph.D. degree in electronic engineering from Xi'an Jiaotong University, Xi'an, in 2004.

She is currently a Professor with the Department of Electronic Engineering, Xi'an University of Technology, Xi'an. Her current research interests include wave propagation, antenna design, and communication signal processing.

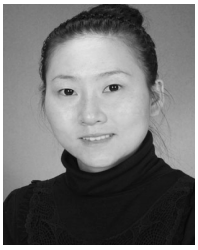

Yu-Rong Pu received the B.S., M.S., and Ph.D. degrees in electronic engineering from the Xi'an University of Technology (XUT), Xi'an, China, in 2004, 2007, and 2013, respectively.

She is currently a Lecturer with the Department of Electronic Engineering, XUT. Her current research interests include computational electromagnetics and wave propagation.

Jin-Sheng Zhang received the M.S. and Ph.D. degrees in navigation, guidance, and control from the Xi'an High-Tech Institute, Xi'an, China, in 2005 and 2009, respectively.

He joined the Control Faculty, Xi'an High-Tech Institute, in 2009, where he founded the Geomagnetic Matching Navigation Research Team in 2004, and is currently an Engineer. His current research interests include geomagnetic matching navigation, simulation and evaluation, and wave propagation.

Li-Li Zhou received the B.S. and M.S. degrees in communication and information systems from the Xi'an University of Technology, Xi'an, China, in 2004 and 2007, respectively, and the Ph.D. degree in electronic science and technology from the Xi'an University of Technology, in 2010.

She is currently an Associate Professor with the Shaanxi University of Science and Technology, Xi'an. Her current research interests include wave propagation and numerical calculation of electromagnetic fields.